



Chain growth mechanism of Fischer–Tropsch synthesis on $\text{Fe}_5\text{C}_2(001)$

Dong-Bo Cao^a, Yong-Wang Li^a, Jianguo Wang^a, Haijun Jiao^{a,b,*}

^a State Key Laboratory of Coal Conversion, Institute of Coal Chemistry, Chinese Academy of Sciences, Taiyuan 030001, PR China

^b Leibniz-Institut für Katalyse e.V. an der Universität Rostock, Albert-Einstein-Strasse 29a, 18059 Rostock, Germany

ARTICLE INFO

Article history:

Received 12 January 2011

Received in revised form 17 June 2011

Accepted 21 June 2011

Available online 28 June 2011

Keywords:

FTS

$\text{Fe}_5\text{C}_2(001)$

DFT

Insertion mechanism

Carbide mechanism

ABSTRACT

The chain growth mechanisms of Fischer–Tropsch synthesis on $\text{Fe}_5\text{C}_2(001)$ were investigated at the levels of density functional theory. On the H_2 and CO co-adsorbed surface, the formation of CH and CCO is the most favored initial steps. The subsequent steps of CCO coupling with C into CCCO and CCO hydrogenation into CCH_2 and CHCH are competitive. Furthermore, CCH from CCH_2 and CHCH dehydrogenation can couple with C to form CCCH. Since chain initiation from CO insertion obeys insertion mechanism, and chain propagation from CCH coupling obeys carbide mechanism, both mechanisms are operative and cooperative in Fischer–Tropsch synthesis. The carburized active surfaces can be regenerated and maintained by CO adsorption on the vacancy site, followed by hydrogenation into surface formyl (CHO) and successive dissociation into surface CH and O. In addition surface O can be hydrogenated into surface OH, and H_2O formation from surface OH disproportionation is energetically more favored than surface OH hydrogenation.

© 2011 Elsevier B.V. All rights reserved.

1. Introduction

Iron-based catalysts are widely used in industrial Fischer–Tropsch synthesis (FTS) [1], which becomes increasingly important especially for liquid fuel production under the background of the predicted lack of crude oil supply. In FTS, iron carbides are the active phases of iron-based catalysts [2–9] and the Hägg iron carbide (Fe_5C_2) is the most representative one. Transmission electron microscopy, Mössbauer spectroscopy and X-ray analysis reveal the responsibility of the highly dispersed Fe_5C_2 for the high FTS activity [3–7]. FTS products are rather complex, including linear paraffins, α -olefins and a small amount of oxygenated compounds such as alcohols, aldehydes, ketones, acids, as well as H_2O and CO_2 [10–12]. Both experimental and theoretical studies have been dedicated to FTS mechanisms, and some insights are outlined below.

Carbide mechanism, originally proposed by Fischer and Tropsch [13], was put forward by Pettit et al. and Biloen et al. [14–17]. They proposed the formation pathway of surface CH_2 and alkyl polymerization scheme. However, the critical point of carbide mechanism is chain initiation, which remains serious debates. Mims et al. [18] used isotopic transient experiment to study high hydrocarbon formation on Ru catalysts, and suggested vinylidene (CH_2C) or ethylidene (CH_3CH) as possible C_2 initiator. Turner [19–25] and Jordan et al., [26,27] showed that C_2 species, derived from

either vinyl-X ($X = \text{Br}, \text{SiR}_3$, etc.) or ethane probes, are incorporated into hydrocarbons over a number of metals, and vinyl (CH_2CH) is involved in initiating polymerization in many experiments [28–32]. Ciobîcă et al. [33,34] studied the FTS mechanism on $\text{Ru}(0001)$ using dynamic Monte Carlo and density functional theory (DFT) method, and found CH as the most likely monomer, as well as CHCH_2 and CHCH_3 as C_2 initiators. On the basis, they [35] proposed the parallel mechanisms of alkylidene (methylene-like) and alkyl (methyl-like) intermediates. Liu et al. [36,37] studied all possible C–C coupling reactions on flat and stepped $\text{Ru}(0001)$ and stepped $\text{Rh}(111)$ using DFT method, and found $\text{C} + \text{CH}$ as the most favored reaction on stepped $\text{Ru}(0001)$ and $\text{Rh}(111)$. Lo and Ziegler [38] studied chain initiation on $\text{Fe}(100)$ with DFT method, and found $\text{C} + \text{CH}_2$ as the most likely reaction pathway and $\text{C} + (\text{CCCH}_2/\text{CCCH}_3)$ as the most favored pathway for chain propagation [39]. On the $\text{Fe}_3\text{C}(100)$ surface, Deng et al. found that surface C_2H_x formation comes from CO insertion into surface carbon followed by C–O bond dissociation and hydrogenation [40]. Although carbide mechanism can explicitly explain the formation of hydrocarbons, it cannot explain the formation of oxygenated products [41].

CO insertion mechanism was proposed by Pichler and Schulz [42], in which $\text{C} + \text{C}$ coupling via CO insertion into adsorbed alkyl with the formation of surface acyl (RCO-) may result in alkyl, alkenes and oxygenates. Emmett et al. [43,44] added radioactive alcohol, ethylene, propionaldehyde and propanol etc. into syngas ($\text{CO} + \text{H}_2$), and found the C_2 – C_{10} products containing radioactive carbon atom, suggesting primary alcohols added as starting nuclei in building up higher hydrocarbons. For CO hydrogenation, the barrier of CHO hydrogenation is 0.45 eV lower than that of dissociation on flat $\text{Co}(0001)$ [45,46]. On flat and stepped $\text{Co}(0001)$, the barrier

* Corresponding author at: Leibniz-Institut für Katalyse e.V. an der Universität Rostock, Albert-Einstein-Strasse 29a, 18059 Rostock, Germany.
Tel.: +49 381 1281 135; fax: +49 381 1281 5000.

E-mail address: haijun.jiao@catalysis.de (H. Jiao).

of CH_2O hydrogenation is 0.09 and 0.40 eV lower than that of dissociation, respectively [45], and the favored product is CH_3OH instead of CH_x . However, the products of ketene (CH_2CO) hydrogenation on $\text{Fe}_5\text{C}_2(001)$ are hydrocarbon instead of ethanol [47]. Therefore, the CO insertion mechanism leading either to oxygenates or to hydrocarbons needs to be understood in detail.

Anderson [48] and Eidus [49] proposed hydroxycarbene mechanism, in which the condensation of two $\text{M}=\text{CHOH}$ group results in CHCOH formation, which can be further hydrogenated to hydrocarbons and oxygenates. Hydroxycarbenes as ligands have been found in transition metal complexes, such as $(\text{CO})_5\text{Cr}=\text{C}(\text{OH})\text{Ph}$ [50] and $(\text{CO})_2\text{Re}=\text{C}(\text{OH})\text{CH}_2\text{CH}_2(\eta^5\text{-C}_5\text{H}_4)$ [51].

Apart from hydrocarbons, H_2O also is a primary product from FTS [52]. It is believed that high H_2O concentration is one factor for oxidation and deactivation of iron carbides [53–56], and therefore understanding H_2O formation and desorption is important for enhancing FTS activity. Michaelides and Hu [57,58] used DFT methods to investigate the microscopic reactions of H_2O formation on $\text{Pt}(111)$, and reported the detailed mechanism. Gong et al. [59] performed DFT calculations to study the mechanism of H_2O formation on flat and stepped $\text{Co}(0001)$ surfaces, and found the H_2O formation is favored at high coverage.

In our theoretical study on chain growth mechanism, both carbide and CO insertion mechanisms on $\text{Fe}_5\text{C}_2(001)$ are considered. Under a wide range of conditions, there are many different intermediates, which may lead to the same products from different pathways. We investigated all possible $\text{C}_1 + \text{C}_1$ couplings for C_2 initiator. On the basis of the favored C_2 formation, the chain growth through $\text{C}_2 + \text{C}_1$ coupling was studied. Furthermore, chain growth mechanism on $\text{Fe}_5\text{C}_2(001)$ was discussed, and compared with chain initiation mechanism on other Fe_xC surfaces. In addition, the mechanism of H_2O formation on $\text{Fe}_5\text{C}_2(001)$ was studied.

2. Methods and models

All calculations were performed at the DFT level using the Cambridge sequential total energy package (CASTEP) [60,61]. Ionic cores were described by ultrasoft pseudopotential [62] and PBE functional [63] (USPP–PBE) and the Kohn–Sham one-electron states were expanded in a plane wave basis set up to 340 eV. A Fermi smearing of 0.1 eV was utilized. Brillouin zone integration was approximated by a sum over special k -points chosen using the

Monkhorst–Pack scheme [64]. The pseudopotential with partial core was used in spin-polarized calculations to include non-linear core corrections [65]. Spin polarization was used to calculate the energies and structures of isolated C_xH_y and $\text{C}_x\text{H}_y\text{O}$. Without counting the adsorbate, the vacuum of the slabs was set to span a range of 10 Å to ensure no significant interaction between the slabs. The convergence criteria for structure optimization and energy calculation were set to: (a) SCF of 2.0×10^{-6} eV/atom; (b) energy of 2.0×10^{-5} eV/atom; (c) displacement of 2.0×10^{-3} Å; (d) force of 0.05 eV/Å (0.25 eV/Å for transition state structure calculation).

The transition state structures were located by using the complete LST/QST [66] method in CASTEP. It starts with linear synchronous transit (LST) maximization, followed by energy minimization in directions conjugate to the reaction pathway. The approximated TS is further used to perform quadratic synchronous transit (QST) maximization. From that point, another conjugate gradient minimization is performed. The cycle is repeated until a stationary point is located. We also calculated the transition state structures of $\text{C}_1 + \text{C}_1$ coupling reactions using the VASP–PAW–PBE method with the convergence criteria for structure optimization and energy calculation: (a) SCF of 1.0×10^{-4} eV; (b) energy of 1×10^{-3} eV; and (c) force of 0.05 eV/Å. Reasonable agreements between VASP–PAW–PBE and CASTEP–USPP–PBE have been found (Supporting Information). Reasonable agreements between VASP and CASTEP also have been found for CH_x hydrogenations on $\text{Fe}_5\text{C}_2(001)$ [67], and ethene epoxidation on two oxidized $\text{Ag}(111)$ surfaces [68].

The vibrational frequencies of adsorbed species and transition state structures were calculated with VASP. This was done with the frozen phonon mode approximation in which the metal atoms are fixed at the relaxed geometries. Due to the large mass difference between Fe and surface carbon species, the vibrations of Fe atoms can be neglected. The Hessian matrix was determined based on a finite difference approach with a step size of 0.02 Å for the displacements of the individual atoms of the adsorbates along each Cartesian coordinate. By diagonalizing the mass-weighted Hessian matrix, the corresponding frequencies and normal modes have been determined. The optimized structures are true energy minimum states with only real frequencies. The optimized transition structures have only one imaginary frequency.

As shown in the side view of $\text{Fe}_5\text{C}_2(001)$ in Fig. 1, in order to compare with carbon hydrogenation [67], we used a model system

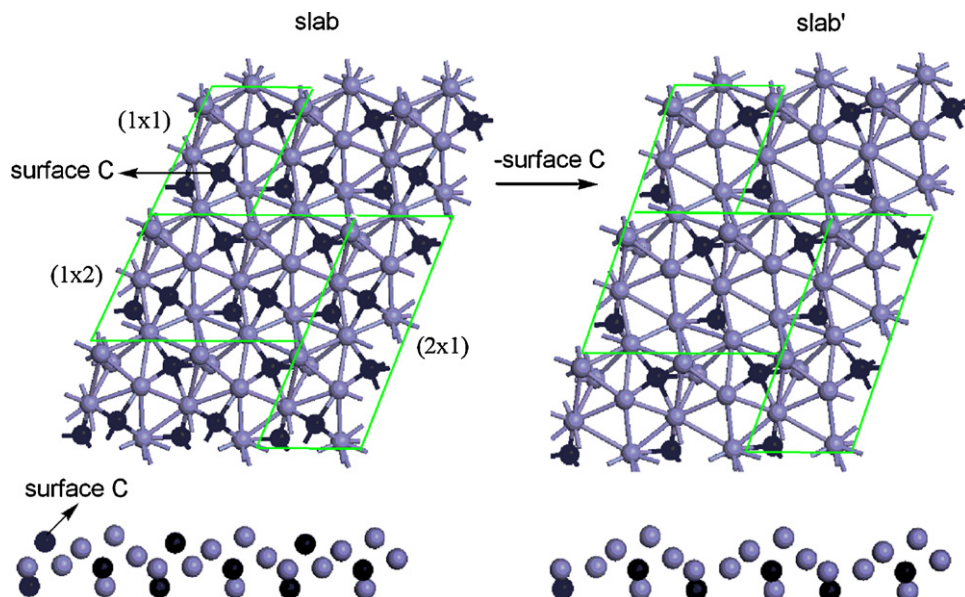


Fig. 1. Top and side views of the $\text{Fe}_5\text{C}_2(001)$ slab.

Download English Version:

<https://daneshyari.com/en/article/66335>

Download Persian Version:

<https://daneshyari.com/article/66335>

[Daneshyari.com](https://daneshyari.com)